STAB'97, Six Int. Conf.on Stability of Ships and Ocean Structures, Pages 81-98, Varna, Bulgaria, September 22-27, 1997.

Reprinted: 08-10-2000
Website: www.shipmotions.nl

Report 1106-P, September 1997,
Delft University of Technology,
Ship Hydromechanics Laboratory,
Mekelweg 2, 2628 CD Delft,
The Netherlands.

Systematic Model Experiments on Flooding of Two Ro-Ro Vessels

J.M.J. Journée (DUT)
H. Vermeer (DGSM)
A.W. Vredeveldt (TNO)

Summary

After the accident of the "Herald of Free Enterprise", research has been started in the Netherlands on the safety of Ro-Ro vessels.
One particular research project of the Ship Hydromechanics Laboratory of the Delft University of Technology concentrates on the ship's motion behaviour and the associated stability characteristics during the intermediate stages of flooding after a collision damage in still water. A mathematical model has been developed, describing the ship's motions due to flooding in the time domain. For validation purposes, a limited number of model experiments have been carried out in the past with two typical Ro-Ro ferries.
After these validations, recently a large number of additional model tests were held on a much more systematic basis. For the two vessels, the effect of the initial metacentric height, the ingress area, the initial angle of heel, the presence of longitudinal bulkheads and cross ducts, the reduction of permeability's and down flooding on capsizing have been examined.
Results of these experiments are presented in this paper. Some important considerations with respect to the intermediate stages of flooding and the initial conditions are given.

1 Introduction

In close co-operation with the Directorate General of Shipping and Maritime Affairs (DGSM), the Delft University of Technology (DUT) and the Netherlands Organization for Applied Scientific Research (TNO) are investigating the dynamic behaviour of ships during a sudden ingress of water after a collision in the side in still water at zero forward speed. During the model experiments on this sudden ingress of water, the roll motions of models of two typical Ro-Ro vessels were measured on time basis.

First, a series of model experiments has been carried out with a 1:50 model of a typical Ro-Ro vessel with a block coefficient of about 0.62, named here "Ferry-62". The transverse bulkhead between the fore and aft engine room was at half-length of the collision gap. From the two midship engine rooms until aft, the ship is subdivided by transverse bulkheads only, over the full breadth of the vessel. Forward of the engine rooms, the ship is subdivided by two longitudinal bulkheads at one-fifth of the breadth from the hull, transverse bulkheads in the side at small

mutual distances and no bulkheads in the center part.
Then, similar experiments have been carried out with a 1:50 model of another typical Ro-Ro vessel with a block coefficient of about 0.72, named here "Ferry-72". This ship has a quite different watertight division. Below the Ro-Ro deck, two longitudinal bulkheads subdivide the ship over the full length at one-fifth of the breadth from the hull. The length of the wing compartments is rather small, while the transverse bulkheads in the center part are located at a much larger distance. To avoid large heeling angles in case of a lateral collision, cross ducts in the double bottom will transfer the incoming seawater to the other side of the vessel (equalizing arrangement).
For both models, the experiments were carried out at three different initial metacentric heights and four different collision gaps.
Vredeveldt and Journée (1991) and Vermeer, Vredeveldt and Journée (1994) have presented the first preliminary results of this research project. Within the framework of contract research of DUT for TNO, some experimental results were reported to TNO in limited distributed technical reports by Journée (1994) and Journee and Onnink (1996).
In the underlying paper, an overview of all experiments is given, while a selected number from this large amount of experimental results is presented and discussed. Also, some comparisons of experimental data with the results of theoretical approximations of the dynamic behaviour of the models during ingress of water are given.

2 Theoretical Approach

Generally, ship motion calculations can be carried out easily with frequency domain programs. But, as a result of the formulation in the frequency domain, any system influencing the behaviour of the vessel should have a linear relation with the motions of the vessel. However, in a lot of cases there are several complications, which perish this linear assumption, for instance the non-linear viscous damping, forces and moments due currents, wind and anchoring, etc. Also, forces and moments due to a collision and the ingress of water afterwards may show a very strong non-linear behaviour.
To include these non-linear effects, it is necessary to formulate the equations of motion in the time domain, which relates instantaneous values of forces, moments and motions.
For this purpose, use has been made of work published by Cummins (1962) and Ogilvie (1964).

2.1 Equations of Motion

The floating vessel is considered to be a linear system with the translational and rotational velocities as input and the reaction forces and moments of the surrounding water as output. The object is supposed to be at rest at time $t = t_0$. Then, during a short time Δt, an impulsive displacement Δx with a constant velocity V is given to this object:

$$\Delta x = V \cdot \Delta t$$

During this impulsive displacement, the water particles will start to move. When assuming that the fluid is inviscid and free of rotation, a velocity potential Φ linear proportional to V, can be defined:

$$\Phi = V \cdot \Psi \quad \text{for: } t_0 < t < t_0 + \Delta t$$

in which Ψ is the normalised velocity potential.
After this impulsive displacement Δx, the water particles are still moving. Because the system is assumed to be linear, the motions of the fluid, described by the velocity potential Φ, are proportional to the impulsive displacement Δx:

$$\Phi = c \cdot \Delta x \quad \text{for: } t > t_0 + \Delta t$$

in which c is the normalised velocity potential.
The impulsive displacement Δx during the period $(t_0, t_0 + \Delta t)$ does not influence the

motions of the fluid during this period only, but also further on in time. This holds that during period $(t_0, t_0 + \Delta t)$ the motions are influenced by the motions before this period too. When the object performs an arbitrarily with time varying motion, this motion can be considered as a succession of small impulsive displacements. Then, the resulting total velocity potential $\Phi(t)$ during the period $(t_n, t_n + \Delta t)$ becomes:

$$\Phi(t) = \sum_{j=1}^{6} \{ V_{j,n} \cdot \Psi_j + \sum_{k=1}^{n} \{ c_j(t_{n-k}, t_{n-k} + \Delta t) \cdot V_{j,k} \cdot \Delta t \} \}$$

in which:

n	number of time steps
t_n	$= t_0 + n \cdot \Delta t$
t_{n-k}	$= t_0 + (n-k) \cdot \Delta t$
$V_{j,n}$	j-th velocity component during period $(t_n, t_n + \Delta t)$
$V_{j,k}$	j-th velocity component during period $(t_{n-k}, t_{n-k} + \Delta t)$
Ψ_j	normalised velocity potential caused by a displacement in direction j during period $(t_n, t_n + \Delta t)$
c_j	normalised velocity potential caused by a displacement in direction j during period $(t_{n-k}, t_{n-k} + \Delta t)$

Letting Δt go to zero, yields:

$$\Phi(t) = \sum_{j=1}^{6} \left\{ \dot{x}_j(t) \cdot \Psi_j + \int_{-\infty}^{t} c_j(t-t) \cdot \dot{x}_j(t) \cdot dt \right\}$$

in which $\dot{x}_j(t)$ is the j-th velocity component at time t.

The pressure in the fluid follows from the linearised equation of Bernoulli:

$$p = -r \frac{\partial \Phi}{\partial t}$$

An integration of these pressures over the wetted surface S of the floating vessel gives the expression for the hydrodynamic reaction forces and moments F_i. With n_i for the generalised directional cosine, F_i becomes:

$$F_i = -\iint_S p \cdot n_i \cdot dS$$

$$= \sum_{j=1}^{6} \left\{ \left(r \iint_S \Psi_j \cdot n_i \cdot dS \right) \cdot \ddot{x}_j(t) + \int_{-\infty}^{t} \left(r \iint_S \frac{\partial c_j(t-t)}{\partial t} \cdot n_i \cdot dS \right) \cdot \dot{x}_j(t) \cdot dt \right\}$$

When defining:

$$A_{i,j} = r \iint_S \Psi_j \cdot n_i \cdot dS$$

$$B_{i,j}(t) = r \iint_S \frac{\partial c_j(t-t)}{\partial t} \cdot n_i \cdot dS$$

the hydrodynamic forces and moments become:

$$F_i = \sum_{j=1}^{6} \left\{ A_{i,j} \cdot \ddot{x}_j(t) + \int_{-\infty}^{t} B_{i,j}(t-t) \cdot \dot{x}_j(t) \cdot dt \right\}$$

for $i = 1,6$

Together with linear restoring spring terms $C_{i,j} \cdot x_j$ and linear external loads $X_i(t)$, Newton's second law of dynamics gives the linear equations of motion in the time domain. When replacing in the damping term t by $t - t$, this term can be written in a more convenient form. Then, the linear equations of motion in the time domain are given by:

$$\sum_{j=1}^{6} \{ [M_{i,j} + A_{i,j}] \cdot \ddot{x}_j(t) + \int_{-\infty}^{t} B_{i,j}(t-t) \cdot \dot{x}_j(t) \cdot dt + C_{i,j} \cdot x_j(t) \} = X_i(t)$$

for $i = 1,6$

in which:

$x_j(t)$ translational or rotational displacement in direction j at time t

$M_{i,j}$ solid mass or inertia coefficient

$A_{i,j}$ hydrodynamic mass or inertia coefficient

$B_{i,j}$ retardation function

$C_{i,j}$ spring coefficient

$X_i(t)$ external load in direction i at time t

Referring to the basic work on this subject by Cummins (1962), these equations of motion are called the Cummins Equations.
The linear restoring spring coefficients $C_{i,j}$ can be determined easily from the underwater geometry and the location of center of gravity G of the vessel, but to determine $A_{i,j}$ and $B_{i,j}$, the velocity potentials Ψ_j and c_j have to be found, which is very complex in the time domain. However, Ogilvie (1964) gives a much more simple method. He found these coefficients from the hydrodynamic mass and damping data, by using results of the linear 2-D or 3-D potential theory in the frequency domain. Relative simple relations are found between $A_{i,j}$ and $B_{i,j}$ and these frequency domain potential coefficients.
In Ogilvie's approach, the vessel is supposed to carry out a harmonic oscillation in the direction j with a normalized amplitude: $x_j = 1 \cdot \cos(wt)$.
After substitution of $x_j, \dot{x}_j$ and $\ddot{x}_j$ in the Cummins equations and comparing the time domain and the frequency domain equations, both with linear terms, he found:

$$A_{i,j} - \frac{1}{w}\int_0^\infty B_{i,j}(t) \cdot \sin(wt) \cdot dt = a_{i,j}(w)$$

$$\int_0^\infty B_{i,j}(t) \cdot \cos(wt) \cdot dt = b_{i,j}(w)$$

$$C_{i,j} = c_{i,j}$$

in which:

$a_{i,j}(w)$ frequency-dependent hydrodynamic mass or inertia coefficient

$b_{i,j}(w)$ frequency-dependent hydrodynamic damping coefficient

$c_{i,j}$ spring coefficient

The first expression with mass terms is valid for any value of w, so also for $w = \infty$. Then the term with the integral, which will be divided by w, vanishes. This gives for the potential mass coefficient:

$$A_{i,j} = a_{i,j}(w = \infty)$$

A Fourier re-transformation of the second expression, with the damping term, gives the retardation function:

$$B_{i,j}(t) = \int_0^\infty b_{i,j}(w) \cdot \cos(wt) \cdot dt$$

It should be mentioned that, with this approach of Ogilvie, the coefficients on the left-hand side of the Cummins equations are still linear. But, the external loads $X_i(t)$ in the right hand side of the equations may have a non-linear behaviour now. Also, non-linear roll damping terms can be added.

2.2 Ingress of Water

The inclining moment is caused by the weight of the floodwater present in the flooded compartments. Throughout the flooding process and the consequential heeling of the vessel both, the amount of water and its location of the center of gravity, vary.
In general, the contribution of the weight of the floodwater to the inclining moment in a particular compartment can be written as:

$$X_4 = rgv \cdot (y\cos f + z\sin f)$$

with (see also Figure 1):

X_4 inclining moment due to weight of water in a compartment

r density of flood water

g acceleration of gravity

v volume of water in considered compartment

y transverse distance between c.o.g. and center line, measured parallel with the ship's base line

z vertical distance between c.o.g. and base line, measured parallel with the ship's center line

f heel angle

The total inclining moment equals the sum of the moments of each flooded compartment.

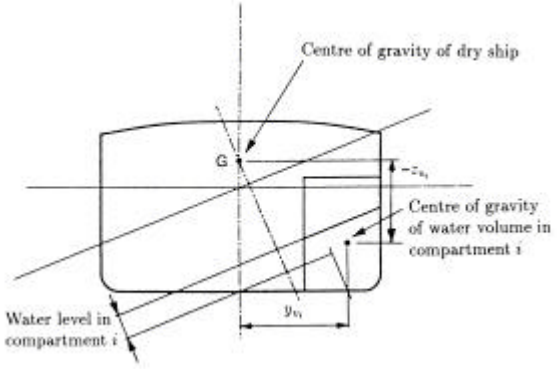

Figure 1 Definition of Symbols

The inclining moment, as described above, refers to the intersection of the ship's center plane and the base plane. The equations of motion of the ship refer to the ship's center of gravity. Therefore, a correction must be applied on this moment:

$$X_{4cog} = X_4 \cdot z_{cog} \cdot \cos f$$

with:

X_{4cog} inclining moment due to weight of water in a compartment with respect to the ship's c.o.g.

z_{cog} vertical distance between c.o.g. and base line, measured parallel with the ship's center line

The amount of floodwater in each compartment depends on the flow of water and flow of air through the damage orifices and the cross-flooding openings. In case of wing compartments, the effect of air vents has to be taken into account.

Water flow can be calculated by applying Bernoulli's law:

$$Q_{water} = A\sqrt{\frac{2 \cdot \Delta P}{r \cdot C}}$$

with:

Q_{water} flow rate between sea and damaged compartment or between adjacent flooded compartment

A flow area

ΔP pressure difference over ingress opening c.q. flooding connection between compartments

C coefficient accounting for flow resistance due to inlet-outlet effects, friction, etc.

For reference, it must be noted that the relation between the coefficient C and the pressure loss coefficient F, as applied in the explanatory notes issued by IMO, can be written as:

$$F = \frac{1}{\sqrt{C}}$$

The airflow can be calculated in a similar manner, however the formula is slightly more complicated due to the compressibility of the air:

$$Q_{air} = A\sqrt{\frac{2 \cdot R \cdot T \cdot \Delta P}{\left|P_f + P_r\right| \cdot C}}$$

with:

Q_{air} flow rate of air through vents

A flow area

R specific gas constant of air

T temperature of air

ΔP pressure difference over air vent

P_f pressure at front of air vent

P_r pressure at rear of air vent

C coefficient accounting for flow resistance due to inlet-outlet effects, friction, etc.

In the case of the ingress openings and the cross-flooding openings two complications occur. The pressure head varies along the height of the opening and the water levels may lie between the upper and lower edge of the opening. Dividing the opening

vertically into a number of strips can cater for these complications. Per strip, it can be decided whether water flow or air flow occurs.

Flow is assumed to stop when the pressure difference over an orifice, flow opening or air vent becomes zero. This happens when water levels in adjacent compartments are equal, which can only occur when these compartments extend vertically above the damaged water line.
In case of a compartment that is located fully below the damaged water line, it is assumed that some air (10% of total compartment capacity) remains trapped inside the compartment. To calculate the air pressure in this trapped volume, the simple gas law is applied:

$$Q_{air} = \frac{R \cdot T}{V_{air}}$$

with:

P_{air} air pressure

V_{air} volume of trapped air

3 Model Experiments

The experiments were carried out in Towing Tank No I of the Ship Hydromechanics Laboratory of the Delft University of Technology. This tank has a length of 142 meter, a breadth of 4.22 meter and a water depth of 2.50 meter. De main dimensions of the full size vessels are given in Table 1. The scale of the two models was 1:50.

		Ferry-62	Ferry-72
Length over all	m	161.00	179.30
Length b.p.p.	m	146.40	169.20
Moulded breadth	m	27.60	24.92
Depth Ro-Ro deck	m	8.10	7.85
Draught	m	6.22	6.08
Clock coefficient	-	0.617	0.717
Volume	m^3	15,500	18,375
1.20 x GM	m	-	1.92
1.00 x GM	m	2.05	1.60
0.80 x GM	m	1.64	1.28
0.60 x GM	m	1.23	-

Table 1 Main Dimensions of Ship

The models were positioned in a transverse manner in the tank at half the length of the tank. The distance between the models and the tank walls was about half a meter and the roll damping waves could propagate over a long distance before they were, after reflection by the tank-ends, diffracted to the model.

3.1 Experimental Set-Up

During the experiments, the roll motions of the model were measured on time basis. The sign of these data corresponds to a right-handed orthogonal coordinate system with the origin in the center of gravity G of the ship, the x-axis in the longitudinal forward direction, the y-axis to port side and the z-axis upwards. This means that heel or roll to starboard is positive and heel or roll to port side, so to the gap, is negative.
The shape of the collision gaps is based on the result of a collision in the side by a ship with a bulbous bow, so a circular gap under the waterline and a triangular gap above the waterline.
The shape and the full-scale dimensions (in mm) of the four collision gaps in the ship are presented in Figure 2. The reference line for the vertical measures in this figure is the ship's base line.

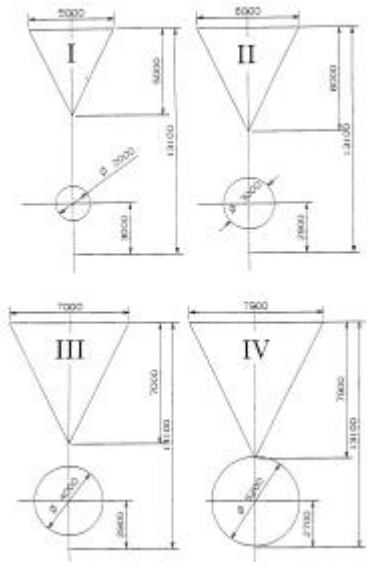

Figure 2 Collision Gaps

The projected areas of these gaps are given in Table 2.

Gap No.	Projected Gap Area		
	Circle (m^2)	Triangle (m^2)	Total (m^2)
I	3.14	12.50	15.64
II	7.07	18.00	25.07
III	12.57	24.50	37.07
IV	21.24	31.20	52.44

Table 2 Areas of Collision Gaps

In the underlying paper, the time histories of the roll angles during the sudden ingress of water into the model are presented. A while before opening the gap the registration was started and a time-reference signal was made available to obtain the instant of opening the gap, $t = 0$.

As soon as the port side gap is opened, water will flow into the model and the port side pressure on the model at the gap will drop down. Still, the effect of the inflooding water has to start. At the starboard side of the model the static water pressure on the model maintains. During a short time, this results in a total hydrostatic force to port side. Because the gap is below the center of gravity, this force causes a small initial roll to starboard. After that, the effect of the flooding water will increase and the model starts to roll to port side.

The experiments were carried out in such a way that the effect of the growth of the gap after the collision with time on the ship motions could be neglected. So, the gap came into existence very sudden; it was nearly a step function. The gap in the hull of the model was closed by a flexible rubber flap, sticked with vaseline to the outside exterior of the hull around the gap.

Without introducing a roll moment, the flap was catapulted away backwards by a spring construction on the model. The release of the sealed spring took place electrically, without touching the model. Experiments on catapulting away the flap from the model without a gap, showed that the discharge of the energy in the spring construction and the slight disturbance of the still water surface by the moving flap did not result in significant ship motions.

Each experiment has been started with a dry model. Water leaked between the flap and the hull via the gap into the model, if any, was pumped away just before starting the experiment. The discretised roll signals were stored in an ASCII-format on diskettes.

To examine the repeatability of the experimental results, a large number of experiments have been carried out twice or even three times.

3.2 Experiments FERRY-62

The bodylines of Ferry-62, the engine rooms with bulkheads and spaces and the location of the collision-gaps are shown in Figure 13. The transverse bulkhead between the engine rooms was at half-length of the gap. Wooden blocks modeled the engines.

The experiments were carried out at three different values for the initial metacentric height. The $\overline{GM}$-values were 2.05 meter (100%), 1.64 meter (80%) and 1.23 meter (60%), respectively.

To obtain roll-damping information, free rolling experiments were carried out with the intact model, so the model with a closed gap, and with the flooded model with gap I.

Then, capsize tests were carried out for the three metacentric heights and the four gaps. To examine the effect of a small initial heel angle, these experiments were repeated with an initial heel.

To examine the effect of the free surface of the flooded water on the Ro-Ro deck, the experiments, which resulted into capsizing, were repeated with a reduced deck width.

3.2.1 Roll Decay Tests

For three metacentric heights of Ferry-62, free rolling experiments were carried out with the intact model, so the model with a

closed gap, and for the flooded model with gap I.

The $\overline{GM}$ value of the intact ship, the heeling moments corresponding to the initial heel angles, the measured natural roll periods T_f and the gyradii for roll of the ship k_{ff}, obtained from T_f, are given in Table 3.

Intact Ship				Ship with Gap I	
$\overline{GM}$		T_f	k_{ff}/B	T_f	k_{ff}/B
(m)	(%)	(s)	(-)	(s)	(-)
2.05	100	15.3	0.395	15.3	0.395
1.64	80	17.0	0.395	19.3	0.445
1.23	60	19.2	0.385	20.4	0.410

Table 3 Still Water Results of Ferry-62

The non-dimensional rolldamping coefficients $k(f_a)$ are presented in Figure 14. The figure shows a very considerable increase of the roll damping during flooding of the engine rooms of the ship. The obstacles in the engine rooms, the simplified wooden models of the engines, mainly cause this.

3.3.2 Capsize Tests

When not taking into account the sinkage during flooding, the Ro-Ro deck of Ferry-62 enters into the water at a heel angle of 7.8 degrees.

The capsize tests were carried out at the three metacentric heights of 1.23, 1.64 and 2.05 meter and the four gaps I, II, III and IV. To examine the effect of a small initial heel angle, these experiments were repeated with initial heel angles of the ship. For the smallest and the largest gap, the results are presented in Figure 16.

Without an initial heel, the ship capsized for all gaps within 7 minutes at the lowest $\overline{GM}$ of 1.23 meter (60%) and survived at the other $\overline{GM}$ values. But with an initial heel angle of about -3 degrees, the ship capsized in all examined cases. At a $\overline{GM}$ of 1.64 meter (80%), the ship capsized when the initial heel angle was about -1 degrees. At the actual $\overline{GM}$ of 2.05 meter, the ship capsized when the initial heel angle was about -3 degrees. The duration of capsizing is strongly depending on the size of the gap; at the largest $\overline{GM}$, 7 minutes for gap I and 1 minute for gap IV.

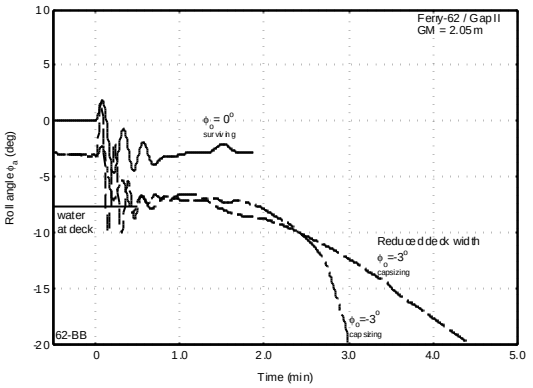

Figure 3 Influence of Reduced Deck Width on Capsizing of Ferry-62

To examine the effect of the free surface of the flooded water on the Ro-Ro deck, those experiments, which resulted into capsizing, were repeated at a reduced deck width. Two beams of hard foam at the Ro-Ro deck at port side and at starboard, with a breadth of 2.50 meter simulated this. This modification did not result into an avoidance of capsizing. However, the time necessary for capsizing will be increased by about 50 per cent. An example is given in Figure 3.

3.3 Experiments FERRY-72

The body lines of Ferry-72, the engine rooms with cross ducts, bulkheads and spaces and the location of the collision-gaps are shown in Figure 16. The transverse bulkhead in the side at half the length of the engine room was in the middle of the gap. During the tests, the engine room was empty.

The experiments were carried out at three different values for the initial metacentric height. The values of $\overline{GM}$-ship were 1.92 meter (120%), 1.60 meter (100%) and 1.28 meter (80%), respectively.

To obtain roll-damping information, free rolling experiments were carried out with the intact model, so the model with closed gap, and with the flooded model with gap I.
Then, a series of capsize tests were carried out for the three metacentric heights and the four gaps. To examine the effect of a small initial heel angle, these experiments were repeated with an initial heel.
To examine the effect of the longitudinal bulkheads, also capsize tests were carried out with the model without these bulkheads, so with engine rooms over the full breadth of the ship.
To examine the effect of the cross duct in the double bottom, capsize tests were carried out with the model with a closed duct.
To examine the effect of water on the Ro-Ro deck, some experiments, which resulted into capsizing, were repeated with deck openings in the Ro-Ro deck.
A few experiments were carried out with the model without a cross duct but with 60 per cent of the volume hard foam in the two port side wing tanks.
Finally, some experiments were carried out in regular beam waves with an amplitude of 1.0 meter.

3.3.1 Roll Decay Tests

For the metacentric heights of Ferry-72, free rolling experiments were carried out with the intact model, so the model with closed gap, and for the flooded model with gap I.

Intact Ship				Ship with Gap I	
$\overline{GM}$		T_f	k_{ff}/B	T_f	k_{ff}/B
(m)	(%)	(s)	(-)	(s)	(-)
1.92	120	14.5	0.400	13.8	0.380
1.60	100	16.2	0.410	15.1	0.380
1.28	80	18.4	0.415	17.3	0.390

Table 4 Still Water Results of Ferry-72

The $\overline{GM}$ value of the intact ship, the heeling moments corresponding to the initial heel angles, the measured natural roll periods T_f and the longitudinal gyradii for roll of the ship k_{ff}, obtained from T_f, are given in Table 4. The non-dimensional roll-damping coefficients $k(f_a)$ are presented in Figure 17.
The figure shows an increase of the roll damping during flooding of water in the ship. The roll damping increases with the metacentric height.

3.3.2 Capsize Tests

When not taking into account the sinkage during flooding, the Ro-Ro deck of Ferry-72 enters into the water at a heel angle of 8.1 degrees.

The capsize tests were carried out at the three metacentric heights of 1.28, 1.60 and 1.92 meter and the four gaps I, II, III and IV. To examine the effect of a small initial heel angle, these experiments were repeated with an initial heel. For the smallest and the largest gap, the results are presented in Figure 18.
Without an initial heel angle, the ship survived in all cases.
With an initial heel angle of -3 degrees and the smallest gap, the ship survived too. But with the largest gap, the ship capsized within 1.5 minutes for the lowest $\overline{GM}$ of 1.28 meter (80%) and it survived at the higher $\overline{GM}$ values.
With an initial heel angle between -4 and -5 degrees, the largest collision gap and the actual $\overline{GM}$ of 1.60 meter, the situation became critical. The ship hesitated to capsize or it capsized within 2.5 minutes.

To examine the effect of the longitudinal bulkheads in the engine room on the safety of the ship, also the time histories of the roll angles were measured during a flooding of the Ferry-72 model without these longitudinal bulkheads, see Figure 4.
After opening the gap with a zero initial heel angle of the ship, an extreme roll angle of -9 degrees was reached and some water entered on the Ro-Ro deck. Then the

ship returned oscillating to an upright position and it seemed to survive. But, due to the water flooding into the engine room, the ship sunk horizontally. As soon as the metacentric height became negative, the ship started to heel to starboard and finally it capsized after 7 minutes.

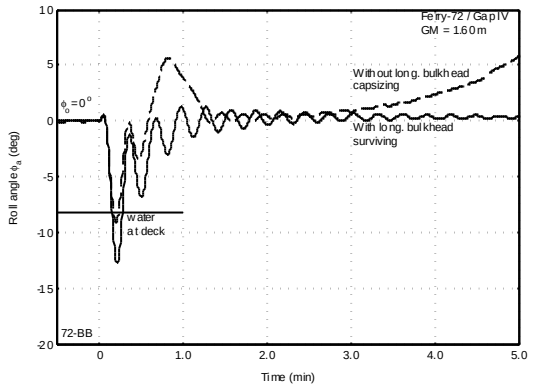

Figure 4 Influence of Longitudinal Bulkhead on Capsizing of Ferry-72

In these model experiments, the ship capsized to starboard because it had a small initial heel to starboard during the horizontal sinkage. This was caused by a small loss of port side mass of the rubber flap and the springs after catapulting away the flap.

To examine the effect of the cross duct in the double bottom, capsize tests were carried out with a closed cross duct. Some results are presented in Figure 5 for the actual $\overline{GM}$ of 1.60 meter and the smallest collision gap.

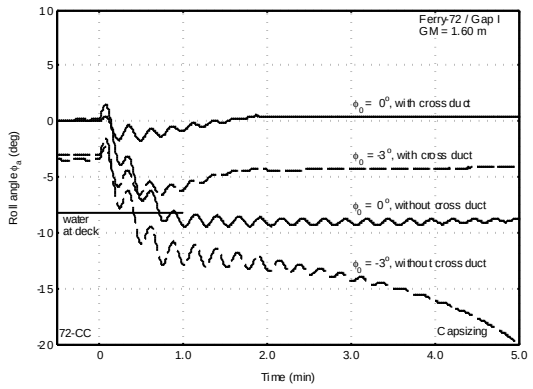

Figure 5 Influence of Cross Duct on Capsizing of Ferry-72

With a cross duct and no initial heel, the ship remained safe. With an initial heel angle of -3 degrees, the ship survived with a final heel angle of -4 degrees, due to a negative initial metacentric height.

With a closed cross duct and no initial heel, the ship survived with a final heel angle of -9 degrees, due to a negative initial metacentric height and the amount of water in the port side wing tanks. Some water entered to the Ro-Ro deck, so this became a very dangerous condition.

With a closed cross duct and an initial heel angle of -3 degrees, the ship capsized in 5 minutes.

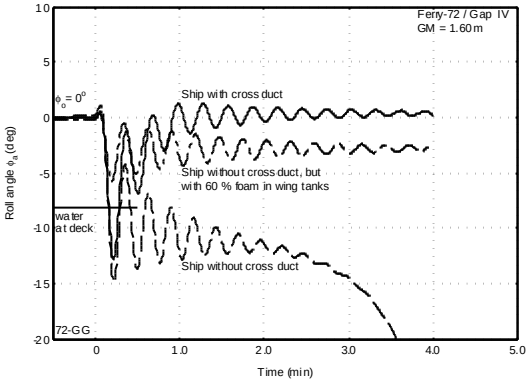

Figure 6 Influence of Permeability in Wing Tank on Capsizing of Ferry-72

A few experiments were carried out with the ship without a cross duct but with 60 per cent of the volume hard foam in the two port side wing tanks. The results are presented in Figure 6 for the actual $\overline{GM}$ of 1.60 meter and the largest collision gap.

As shown before, the ship remained safe with a cross duct. Without a cross duct, the ship capsized after 3.5 minutes. But, with 60 volume per cent hard foam in the port side wing tanks, the ship remained safe with a final heel angle of -3 degrees.

To examine the effect of water on the Ro-Ro deck, some experiments, which resulted into capsizing or nearly capsizing, were repeated with deck openings in the Ro-Ro deck, through which water at deck could flow downwards. For the lowest

metacentric height and collision gap III, an example of the results is given in Figure 7.

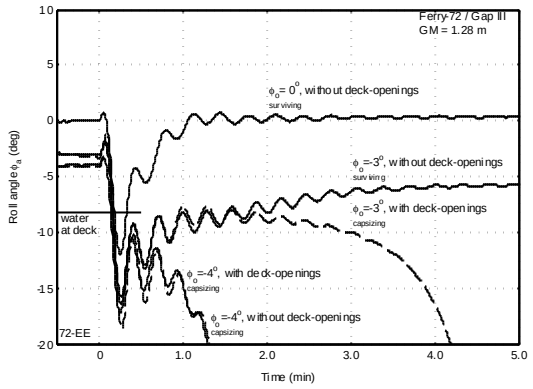

Figure 7 Influence of Deck Openings on Capsizing of Ferry-72

Without deck openings and no initial heel, the ship remained safe.
Without deck openings and with an initial heel angle of -3 degrees, the ship survived with a final heel angle of -6 degrees, due to a reduced metacentric height.
With deck openings and with an initial heel angle of -3 degrees, the ship capsized after 4 minutes.
Without and with deck openings and an initial heel angle of -4 degrees, the ship capsized within 1.5 minutes.

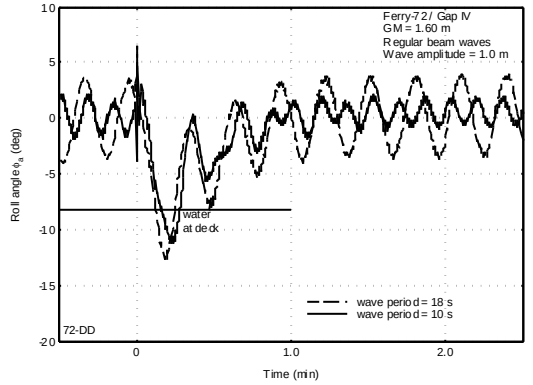

Figure 8 Influence of Regular Beam Waves on Capsizing of Ferry-72

Finally, experiments were carried out in regular beam waves with an amplitude of 1.0 meter and a wide range of wave periods. Figure 8 presents some results for the actual $\overline{GM}$ of 1.60 meter, the largest collision gap and two regular wave periods. In all wave conditions the ship remained safe.

4 Validation of Theories

The calculation method, as described in sections 2.1 and 2.2 and as implemented in the computer simulation program DYNING (DYNamic INGress of water), has been subjected to validation against model experiments. Unfortunately, no full-scale test data could be obtained until now. As a consequence, any scaling effects are ignored.
Prior to validation against some of the tests as presented in this paper, a preliminary validation has been carried out based on tests with a pontoon type model of 3.00 m length, 2.10 m width and a draught of 0.625 m. The model was fitted with opposite wing tanks, connected with a cross duct. The results of this validation were satisfactory, as published in the past by Vredeveldt and Journée (1991).
Figure 9 and Figure 10 show calculated and measured angles of roll for Ferry-62 due to sudden water ingress, obtained during a feasibility study of the tests described in this paper. These first model experiments on Ferry-62 are given in a limited distributed report by Journée (1994). Figure 9 refers to a realistic $\overline{GM}$ value of 2.05 meter. Figure 10 shows results for a $\overline{GM}$ of 1.64 meter, which would normally not be accepted during operation.

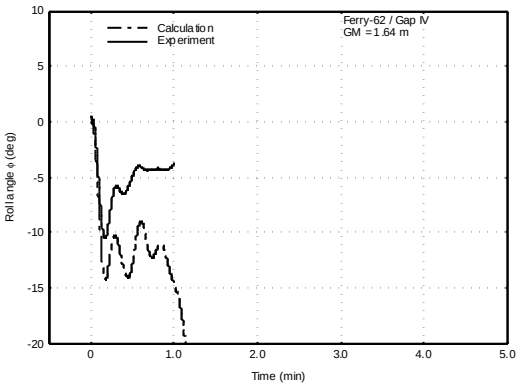

Figure 9 Measured and Calculated Roll of Ferry-62 for GM = 1.64 m

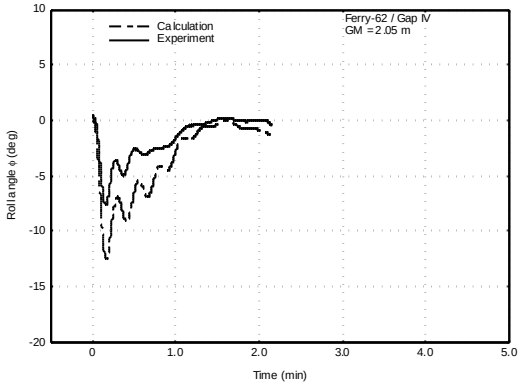

Figure 10 Measured and Calculated Roll of Ferry-62 for GM = 2.05 m

As can be seen, the calculated time span till maximum heel correlates well with the measured value. However, the calculated angle of heel is larger than the measured value. Moreover, in this case the calculated decay is much smaller than measured. The best suggestion for an explanation of both differences is that the sloshing effect of the floodwater is too large to be neglected. However, it should be remarked that the chosen test case for the Ferry-62 does not take into account the presence of piping in the engine room, which is expected to have a large damping effect on the sloshing motions. Making any sensible remarks on this aspect seems impossible on the basis of theory and model experiments alone.

Figure 11 and Figure 12 show calculated and measured roll motions for the Ferry-72 due to sudden water ingress as presented in this paper.

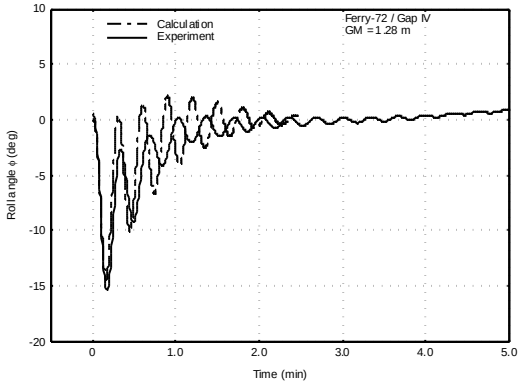

Figure 11 Measured and Calculated Roll of Ferry-72 for GM = 1.28 m

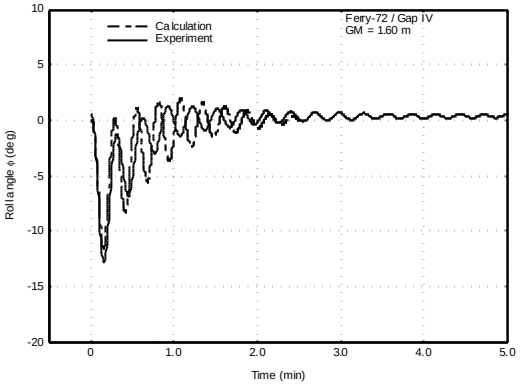

Figure 12 Measured and Calculated Roll of Ferry-72 for GM = 1.60 m

Figure 11 refers to a $\overline{GM}$ value of 1.60 meter, which is realistic for this ship. Figure 12 refers to a $\overline{GM}$ of 1.28 meter, which is beyond operational limits.

In this case calculated and predicted angle of heel and time required till maximum heel show a reasonable resemblance with measured values. However, again calculated motion decay is smaller than measured, although the difference is much smaller than in case of the Ferry-62.

The results support the suggestion that sloshing plays a significant role. In the test case of the Ferry-72 the sloshing motions of the floodwater will be much smaller than in case of the Ferry-62 because of the limited tank width of the flooded compartment, $1/5 \cdot B$ instead of $3/5 \cdot B$ in case of the Ferry-62.

5 Conclusions

From the experiments with the Ferry-62 and the Ferry-72 some conclusions may be drawn:

1. The roll decay tests show that obstacles like engines will cause a considerable increase of the roll damping of a ship in a flooded condition.
2. The experiments described in this paper showed that certain combinations of the $\overline{GM}$ value, the size of the collision gap and the magnitude of the initial heel angle can

result in flooding of water on the Ro-Ro deck. As soon as this happens, a large probability on capsizing of the ship comes into existence.

3. It was found that the two longitudinal bulkheads in the engine room area of Ferry-72 were of paramount importance. Without these two bulkheads this ship will capsize, even at an upright initial condition. With an initial heel angle of -3 degrees, Ferry-72 with these bulkheads will survive while Ferry-62, not equipped with this type of subdivision, will capsize.
4. A cross duct has a very positive effect on the probability of survival of the ship. The restoring roll moment decreases, because water can flow in a short time from one side of the ship to the other side. Fitting obstacles in these ducts, like for instance pipes, should be avoided as far as possible.
5. The permeability of the wing tanks has a large effect on the probability of survival of the ship.
6. Deck openings in the Ro-Ro deck, through which water at deck can flow downwards, seemed to have a small negative effect on the safety of the ship. However, only one single case has been tested and the location of the deck openings is very important. So, this aspect needs further research.

For the Ferry-72 model the sloshing motions of the floodwater were much smaller than for the Ferry-62 model, because of the limited tank width of the flooded compartment of the first mentioned model. Sloshing was not included in the computer simulations in this paper. From the results of the simulations it appeared that a significant role of sloshing could be expected in the case of wide flooded compartments.

If the case of not too wide flooded compartments (Ferry-72), the roll motions predicted by the computer simulation program DYNING are in a satisfactory agreement with the experimental data. But in the case of wide flooded compartments (Ferry-62) the agreement was very poor. So, also this aspect needs further research.

6 Acknowledgements

The authors are very much indebted to Mr. R. Onnink of the Delft Ship Hydromechanics Laboratory for carrying out the large amount of experiments with the two Ro-Ro models and to Mr. J.J. Uwland of TNO for carrying out the calculations.

Also, the practical advises and comments during this project of Ir. E. Vossnack, former head of the Nedlloyd Newbuilding Department, are very much appreciated.

7 References

Cummins (1962)
W.E. Cummins, *The Impulse Response Function and Ship Motions*, Symp. on Ship Theory, January 25-27, 1962, Hamburg, Germany, Schiffstechnik, Volume 9, Pages 101-109.

Ikeda, Himeno and Tanaka (1978)
Y. Ikeda, Y. Himeno and N. Tanaka, *A Prediction Method for Ship Rolling*, Report 00405, 1978, Department of Naval Architecture, University of Osaka Prefecture, Japan.

Journée (1994)
J.M.J. Journée, *Experiments on the Dynamic Behaviour of Ferry-62 during a Sudden Ingress of Water*, Report 1014-O (limited distribution), Ship Hydro-mechanics Laboratory, Delft University of Technology, The Netherlands.

Journée and Onnink (1996)
J.M.J. Journée and R. Onnink, *Experiments on the Dynamic Behaviour of Ferry-72 during a Sudden Ingress of Water*, Report 1034-O (limited distribution), Ship Hydromechanics Laboratory, Delft University of Technology, The Netherlands.

Ogilvie (1964)
T. Ogilvie, *Recent Progress Towards the Understanding and Prediction of Ship Motions,* Proceedings of Fifth Symposium on Naval Hydrodynamics, Pages 3-128, September 10-12, 1964, Bergen, Norway.

Vermeer, Vredeveldt and Journée (1994)
H. Vermeer, A.W. Vredeveldt and J.M.J. Journée, *Mathematical Modeling of Motions and Damaged Stability of Ro-Ro Ships in the Intermediate Stages of Flooding,* STAB'94 Conference, Melbourne, U.S.A.

Vredeveldt and Journée (1991)
A.W. Vredeveldt and J.M.J. Journée, *Roll Motions of Ships due to Sudden Water Ingress, Calculations and Experiments,* International Conference on Ro-Ro Safety and Vulnerability - the Way Ahead, April 17-19, 1991, London, U.K.

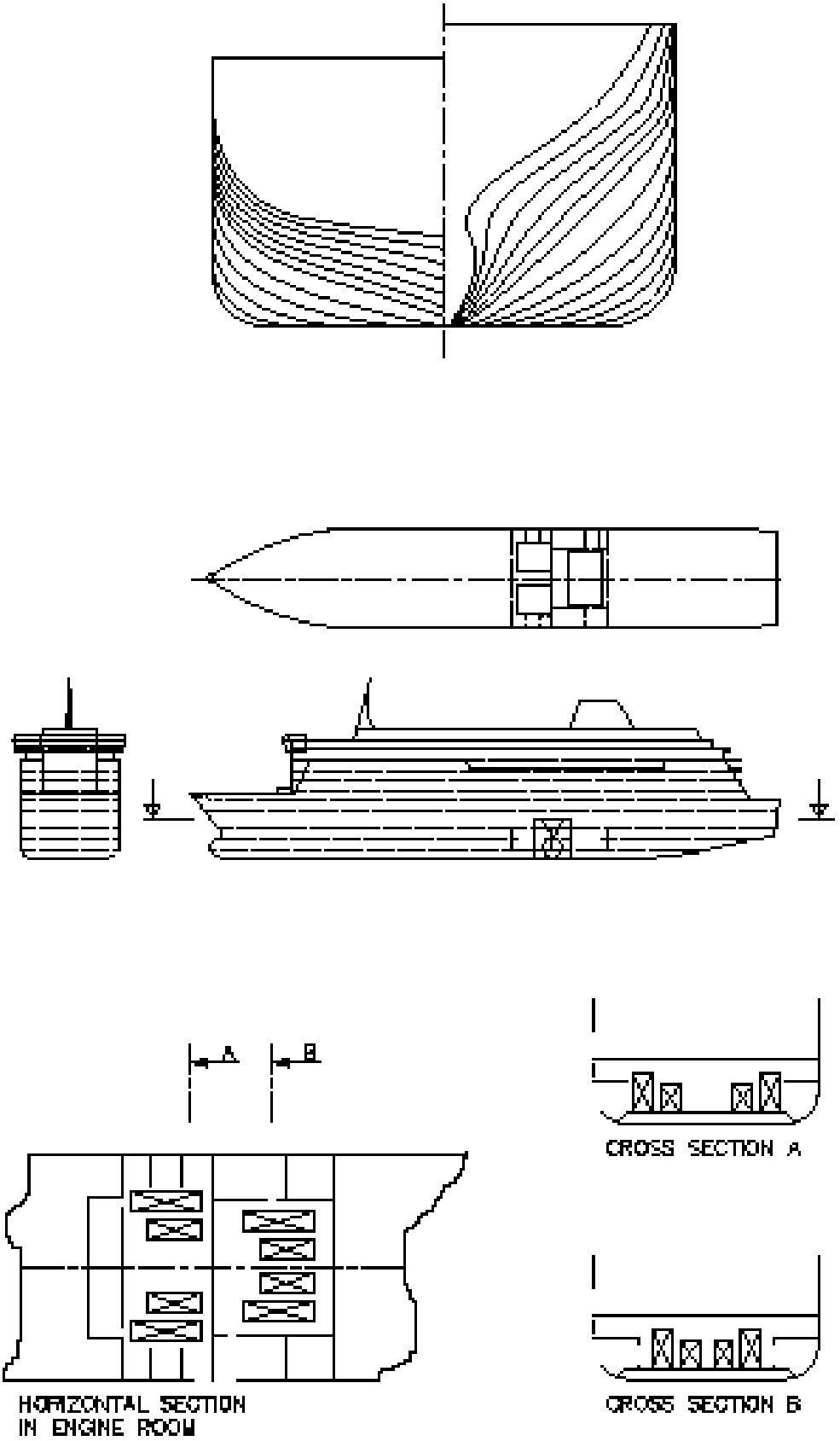

Figure 13 Lines Plan and Engine Room of Ferry-62

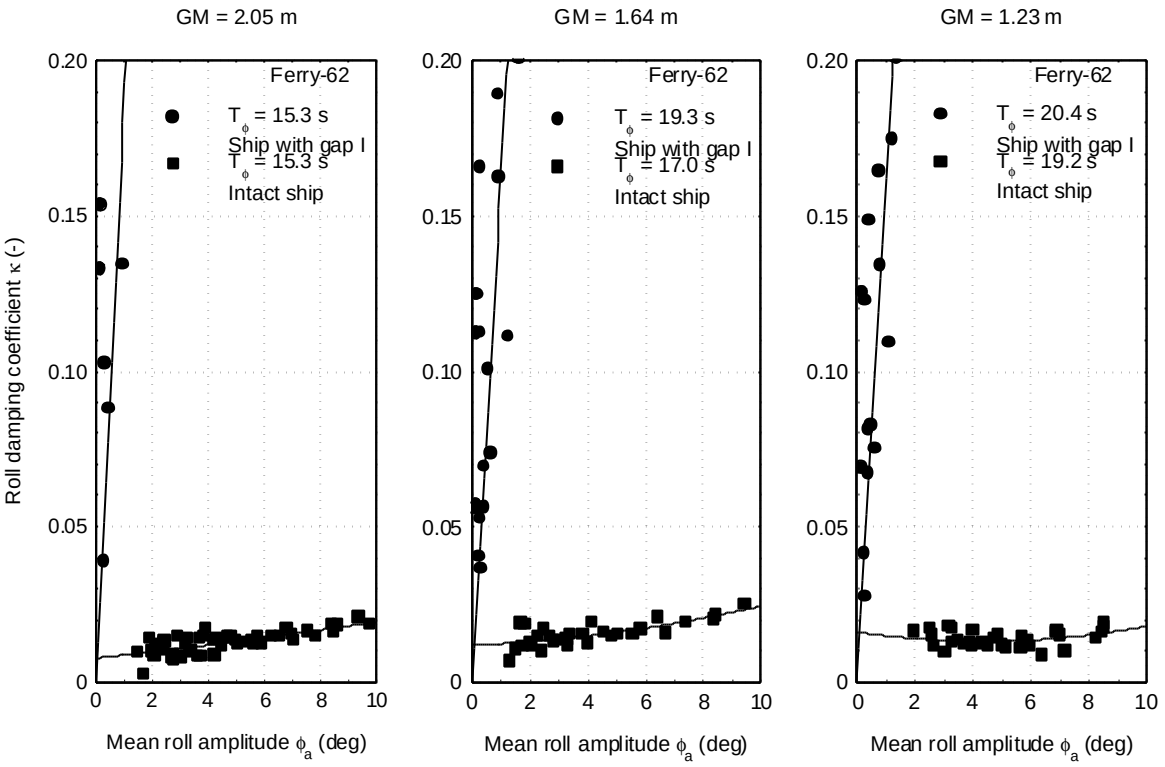

Figure 14 Non-dimensional Roll Damping Coefficients of Ferry-62

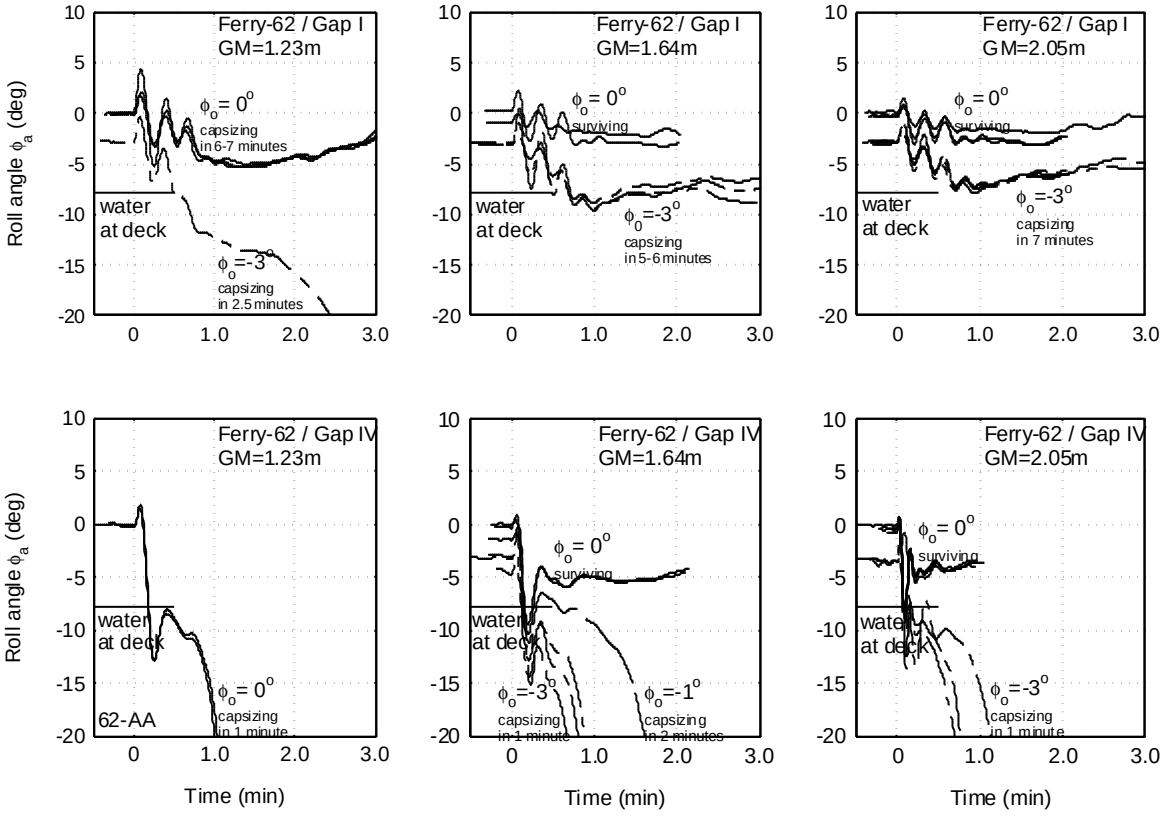

Figure 15 Some Results of Capsize Experiments with Ferry-62

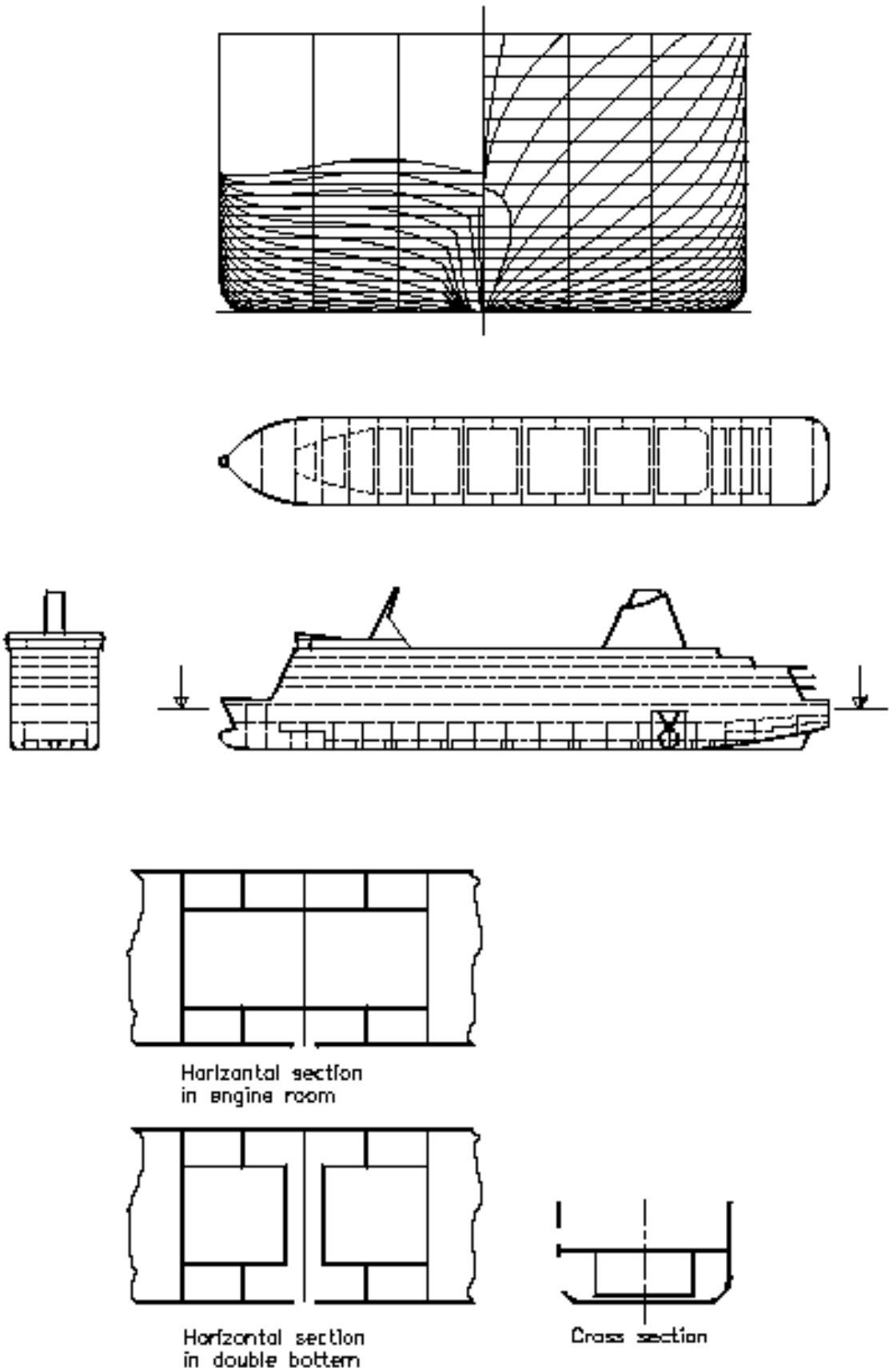

Figure 16 Lines Plan and Engine Room of Ferry-72

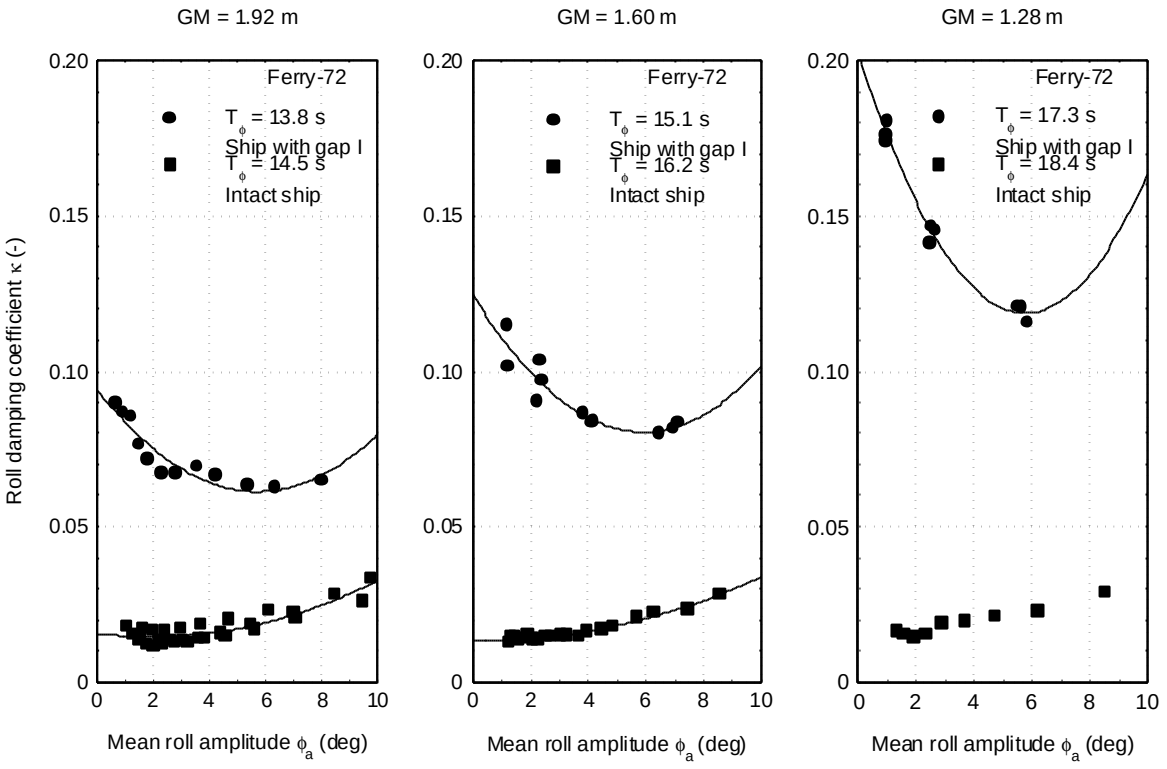

Figure 17 Non-dimensional Roll damping Coefficients of Ferry-72

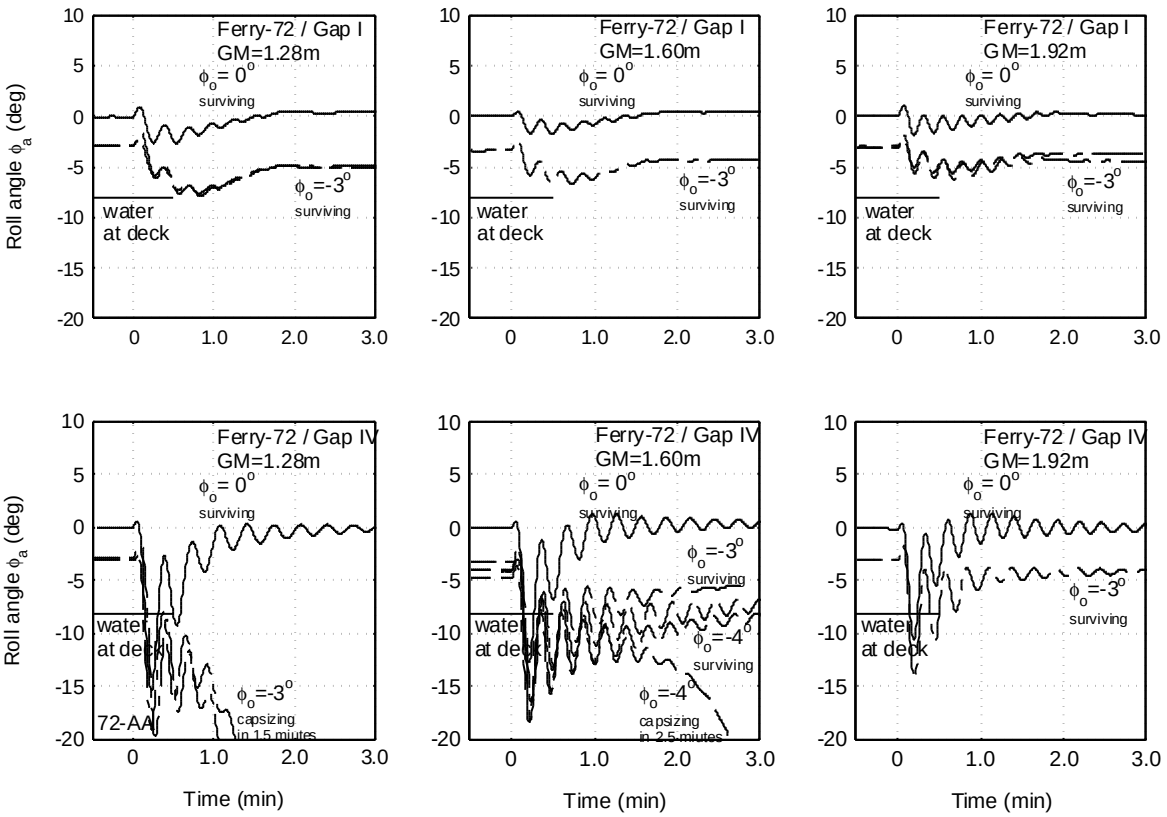

Figure 18 Some Results of Capsize Experiments with Ferry-72